PHYSICAL REVIEW A VOLUME 16, NUMBER 4 OCTOBER 1977

Molecular effects in charge-state distributions from dissociative collisions of 300–900-keV H_2^+ ions

D. Nir, B. Rosner, A. Mann, and D. Maor
Department of Physics, Technion-Israel Institute of Technology, Haifa, Israel
(Received 10 February 1977)

Charge states of the two fragments produced in a single dissociative collision of H_2^+ (energy range 300 to 900 keV) in gas targets (H_2, He, air, and Ar) have been determined by coincidence techniques. The dependence of the charge-state distributions on the energy of the incoming H_2^+ and on the pressure of the various targets has been determined. Correlation coefficients between the distributions are deduced, and a simple model for the dissociation is discussed.

I. INTRODUCTION

The dissociation processes of H_2^+ are of great interest because of their implications for obtaining H^+ for beams in various accelerators, H^- for tandem accelerators, and H^0 for injection in tokamak fusion reactors, etc. A discussion of their importance and of the cross sections for charge exchange in an atomic hydrogen beam may be found in many works (see, e.g., Tawara and Russek[1]). Total cross sections for various dissociation channels in gas targets and their energy dependence were measured in the range of tens[2] of keV and of hundreds of keV.[3] At the lower energies the angular and velocity distributions of the fragments were also measured. The results in this low regime are in accord with a model in which dissociation occurs via electronic excitation of H_2^+ into autodissociative states. The theoretical calculations were carried out separately for each dissociation channel and did not consider relationships among the various channels.[4]

The charge states of fragments from H_2^+ transmitted through foils were measured recently.[5] They were found to differ from those of H^+ passing through the same foil. This difference was attributed to molecular effects.[5]

The purpose of the present work was to measure and correlate all the heavy dissociation fragments produced in a single collision of H_2^+. This was carried out by using electrostatic separation and electronic coincidence techniques.

Our data (together with data obtained from a compilation of experimental dissociation cross sections[3]) are presented in terms of charge-state distributions instead of cross sections. This form of presentation throws into sharp relief the charge-state effects. It emphasizes the correlations among the various charge states and enables a comparison with charge states obtained in foils. Finally, it should be noted that the H_2^+ dissociation problem is amenable to theoretical treatment because the molecular structure of H_2^+ is well known theoretically. However, other molecular ions, such as H_3^+, N_2^+, O_2^+, are far more difficult to treat theoretically. It is therefore advantageous to treat the H_2^+ within a framework which can be easily extended to the analysis of charge states of more complicated ions.

Equations for the dissociation process are developed and solved for two extreme cases: (i) collisions in a thick foil; (ii) collisions in which one of the proton fragments of H_2^+ is merely a spectator (i.e., it cannot exchange charge with the target). Two forms of correlation factors are tested and both indicate the existence of correlations. A simple semiempirical model using geometrical considerations for the dissociation process is developed. The various dissociation processes are discussed in terms of this model.

II. EXPERIMENTAL SYSTEM

An H_2^+ beam in the energy range 300–900 keV was obtained from a J. N. Van de Graaff accelerator. The beam was analyzed magnetically, resulting in a clean H_2^+ beam with an energy defined to within a few keV. Its intensity was reduced to 1000 particle/sec by means of a slit in front of the magnet. The beam was stable, with a diameter of 1 mm and angular dispersion less than 0.1°. The length of the dissociation chamber was 5 cm and it had a diameter of 5 cm. A differential pumping system was arranged on both sides of the chamber. The ratio of pressures between the inside and outside was 100:1, approximately. A 1-mm entrance aperture and a 3-mm exit aperture permitted fragments scattered at angles up to about 2° to pass out of the chamber.

The undissociated ions and the neutral and charged fragments were separated by an electrostatic deflector and counted by a system of three detectors at the appropriate angles. The geometric arrangement is shown in Fig. 1. The distance of

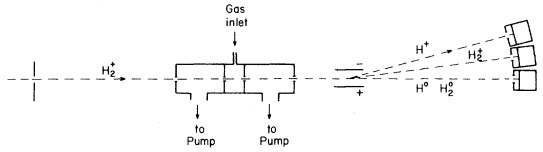

FIG. 1. Experimental arrangement for detecting charge states of pairs of molecular fragments. It includes a differentially pumped dissociation chamber, an electrostatic deflector, and a set of detectors.

the detectors from the dissociation chamber was 900 mm. The two fragments's detectors are Si surface barrier detectors (300 mm^2 active area) and have collimators 19 mm in diameter. The detector of the undissociated beam is a Si surface barrier detector (50 mm^2 active area) and has a collimator 6 mm in diameter.

The signals from the undissociated beam were counted with a fast scaler. The signals from the detected neutral and charged fragments were matched in timing, and were added in a summing amplifier (alternative with advantages to a coincidence unit). The amplification gains of the two electric branches of the H^0 and H^+ detectors were set to 3:2, thus the sum signals of different events

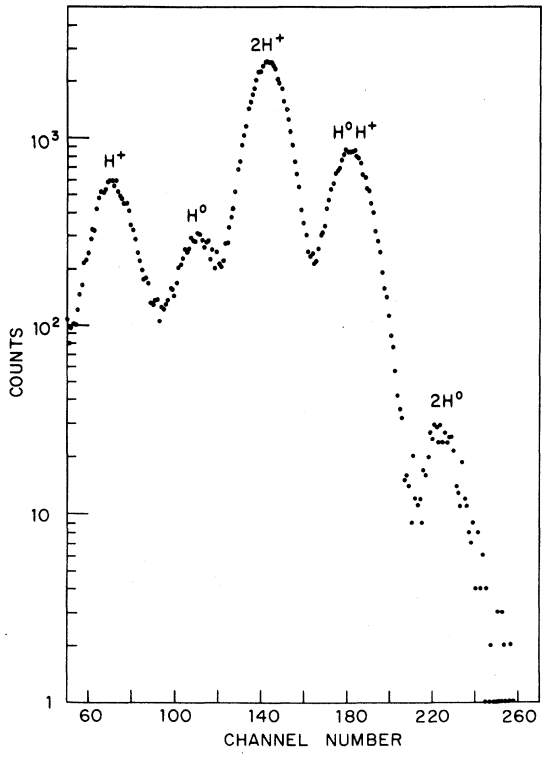

FIG. 2. Sum spectrum of the detectors for neutral particles and H^+. Seen in the spectrum are peaks corresponding to H^+, H^0, $2H^+$, H^0H^+, and $2H^0$.

were not overlapping. Five peaks appeared in the MCA, which described the counting of H^+, H^0, $2H^+$, H^0H^+, $2H^0$. These peaks are shown in Fig. 2. The probability for H^- fragments in this energy range is very small.[3] Their detection in addition to the other fragments would require a much more complicated experimental system.

Various checks on the accuracy and the consistency of the measurements were carried out. The 0° direction of the beam was determined for every experiment, using a small aperture for the detector, to ensure proper experimental geometry. The deflection voltage was set at the point at which the counting ratio $2H^+/H^+$ was maximal. The dependence of the ratio H_2^+/H^0 on the deflection voltage was also checked to ensure proper geometry. The dissociation caused by residual gases and scattering from the slits was checked for each run and did not exceed 1%. This percentage increased as expected with the pressure of the gas in the dissociation chamber, probably due to additional dissociation in the region before the chamber. However, this additional dissociation did not disturb the measurements as it contributed only to the peaks of a single particle H^0 or H^+. The separation between the peaks corresponding to different events was usually better than the ratio 5:1 of peak to valley as seen in Fig. 2. The experiments were performed at low pressures in a region where single collisions were by far most probable. As we see in Ref. 1, the charge exchange cross section is not larger than the dissociation cross section. In the experiments the percentage of the dissociated ions was kept below 10–15%. Therefore multiple collisions and charge exchange are improbable. The dependence of the charge states on the pressure was measured in this work and the experiment was carried out at a region below the point at which rapid changes were observed. Extrapolation of charge state curves to zero pressure does not change the values of the charge states by more than 2%. The statistical error was about 2%, and the probable error in the measured values is 3%.

III. EXPERIMENTAL RESULTS

By adding the signals from the two detectors of the fragments and matching the timing and amplification gains, five peaks were observed. These peaks correspond to the detection of fragment groups H^+, H^0, $2H^+$, H^0H^+, $2H^0$. The H^0 and H^+ come mostly from the beam additional dissociation before the dissociation chamber as discussed above. Their dependence on the target gas pressure differs from that of the peaks corresponding to dissociation products. It should be emphasized that the apertures and geometry allowed the en-

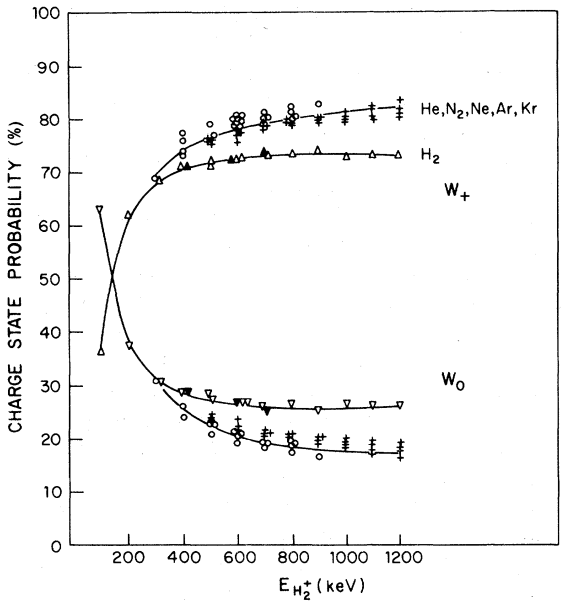

FIG. 3. Charge-state probabilities of H_2^+ fragments versus projectile energy. W_+ is the ratio of positively charged fragments to total number of fragments and W_0 is the ratio of neutral fragments to total number. For various gas targets the results are very close: present data (○), Ref. 3 (+). For a H_2 target there is a remarkable difference (the lines are merely guide for the eye). Present data (▲), Ref. 3 (△).

trance of all outgoing fragments at angles up to 0.7°, whereas measurements show that the fragments, including those undergoing "Coulomb explosion" (scattering due to Coulomb repulsion of the charged fragments), do not scatter to more than 0.3°.

The areas of the peaks of $2H^0$, H^0H^+, $2H^+$ events divided by their sum give the normalized probabilities denoted W_{00}, W_{0+}, and W_{++}, respectively. The fraction of positive fragments out of all fragments is denoted by W_+ and is equal to $W_{++}+\frac{1}{2}W_{0+}$. The neutral fraction denoted W_0 is equal to $W_{00}+\frac{1}{2}W_{0+}$.

Figure 3 shows the dependence of W_+ and W_0 on the incoming H_2^+ energy. The measured points coincide with those deduced from cross-section measurements.[3] The results for He, Ar, and air are very similar (W_+ for an Ar target is slightly higher), and the differences are within the experimental errors. The percentage of neutral particles decreases from 30 to 17%. On the other hand, W_0 in the dissociation of H_2^+ on H_2 is very near to 25%, and these experimental results form a distinctly different curve.

Figure 4 shows the probabilities for the various dissociation channels: W_{00}, W_{0+}, and W_{++} measured for several gas targets at various energies. The results for the targets (which do not include H_2) are similar, although the W_{++} for Ar is a little bit higher. W_{00} drops by an order of magnitude in this energy region, whereas W_{0+} goes down from 45 to 33%. W_{++} goes up from 47 to 67%. An extrapolation of the curves indicates crossing of the W_{0+} and W_{++} curves at an H_2^+ ion velocity of 5×10^8 cm/sec. The solid lines are the predictions of the model discussed below.

Figure 5 shows the dissociation channels on an H_2 gas target. At energies above 100 keV, W_{0+} is more than 50% and decreasing, whereas W_{++} is lower than 50% and slowly rising. It seems, however, that the curves do not cross. W_{00} decreases very fast from 44% at 100 keV to 1% at 500 keV, and becomes negligible. The solid lines are the prediction of the model discussed below.

Figure 6 shows the dependence of the charge states on the pressure of the gas target (air in this case). As expected, the W_{00} and W_{0+} curves decrease, whereas W_{++} increases, towards equilibrium values. The percentage of dissociation is also shown in the figure, since the pressure was measured by a cold cathode gauge at a point outside the chamber and was calibrated only approximately. The effective thickness of the gas target at maximum pressure is approximately 0.2 $\mu g/cm^2$.

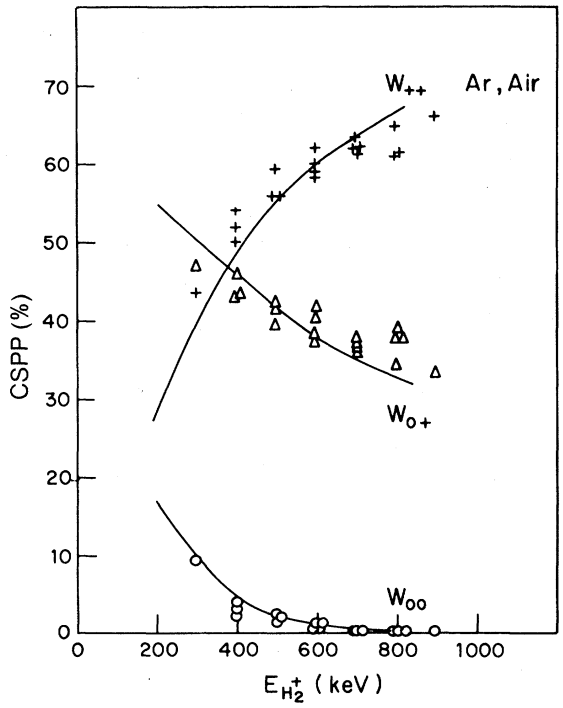

FIG. 4. Charge-state probabilities of pairs (CSPP) of fragments: W_{++}—two charged fragments, W_{00}—two neutrals, W_{0+}—one neutral and one charged. The lines are the prediction of the model as discussed in the text.

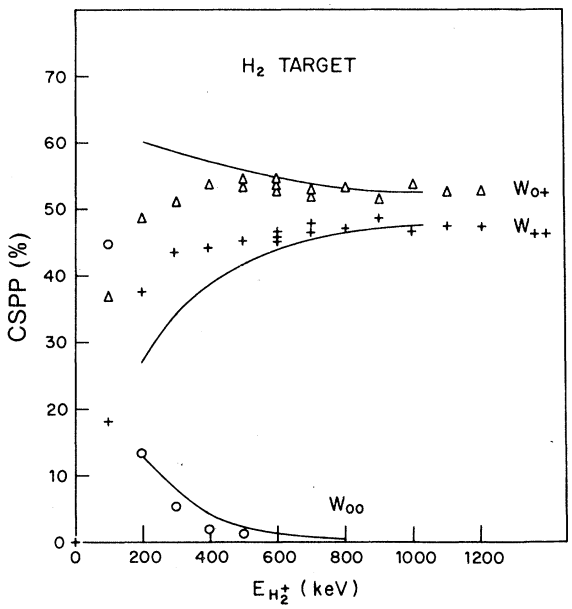

FIG. 5. Charge-state probabilities of pairs (CSPP) of fragments in a hydrogen gas target. Notation as in Fig. 4. The lines are the prediction of the model as discussed in the text.

This figure shows also that the charge exchange cross section is not high.

IV. DISCUSSION AND INTERPRETATION OF THE RESULTS

A. Dissociation process at high energies

We have observed several effects in the charge states of collisionally dissociated H_2^+ fragments. The charge states after collisions in He, air, and Ar are similar, and therefore it is reasonable to assume that the dissociation process is similar. In an H_2 target the results are different from all the others, and the dissociation process is also probably different.

An accepted model for the analysis of the dissociation of H_2^+ is excitation to autoionization states. There is little doubt that this is indeed the main mechanism at low energies. This is shown by the angular distributions and velocity profiles of the fragments[2] and by many theoretical calculations.[4] When the velocity of the incoming ion increases, the situation is no longer so clear. Molecular processes, such as electron capture and formation of H_2^0 or $H^0 + H^0$, decrease rather fast and become negligible at 400 keV. The similarity seen at low energies between the angular distribution of the fragments in the H^0H^+ and $2H^+$ dissociation channels[2] disappears at higher energies. The $2H^+$ distribution is predicted by the Coulomb explosion, whereas the H^0H^+ branch has a Gaussian distribution, as is shown by our measurements. Another indication of the diminishing importance of molecular processes at higher energies is the equality of the electron-loss cross sections for atomic hydrogen and H_2^+ found in Ref. 6. Experiments studying the electrons emitted in the dissociation of H_2^+ (Ref. 7) have also shown that in our energy range the two protons and the electron behave as three independent particles. Furthermore, a detailed calculation may be useful for H_2^+, for which the wave functions are well known. It is not very useful for heavier or more complicated molecules, such as N_2^+, O_2^+, H_3^+. Also, the behavior of charge state produced after transmission through a foil[5] cannot be described by such calculations. We therefore attempt to describe the collisionally produced H_2^+ fragments by focusing attention on the charge states, instead of dealing with the independent dissociation channels. In this way, useful expressions can be obtained that may be extended to heavier and more complicated molecules.

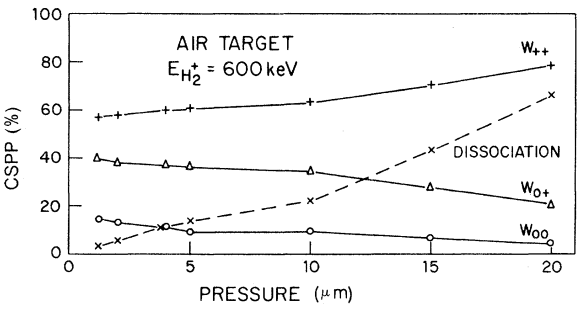

FIG. 6. Charge-state dependence on the target gas pressure (air target). Notation as in Fig. 4. The dashed line shows the dissociated fraction of the molecular beam.

B. Equation for the dissociation process

Let us consider a simple model for the description of the charge-state distributions. Its basic assumptions are that (i) upon approaching the target atom, the electron has an equal probability of being with each proton fragment and it cannot hop from one to the other during the dissociation process; (ii) the charge state of a fragment may be changed only inside a well-defined region around the target atom, which we call the dissociation region; (iii) the final charge state of a fragment depends on the original one, and may be influenced by the presence of nearby fragments. According to the results on cross sections for electrons emitted in the dissociation of H_2^+ (Ref. 7), the chemical bond determines essentially the distri-

bution of the electron before dissociation. The velocity of the H_2^+ electron in the H_2^+ frame is much smaller than the translational velocity of the ion itself. These observations form the basis for assumption (i).

Using (i)–(iii), we can obtain expressions for the charge-state distributions, as follows. Assume a probability P_{1C} for electron capture by the first fragment (when it is without an electron), probability P_{2L} for electron loss by the second fragment (when the electron is attached to it), etc. Then we have

$$W_{++} = \langle \tfrac{1}{2}(1 - P_{1C})P_{2L} \rangle + \langle \tfrac{1}{2}(1 - P_{2C})P_{1L} \rangle , \tag{4.1}$$

$$W_{0+} = \langle \tfrac{1}{2}(1 - P_{1C})(1 - P_{2L}) + \tfrac{1}{2}P_{1C}P_{2L} \rangle + \langle \tfrac{1}{2}(1 - P_{2C})(1 - P_{1L}) + \tfrac{1}{2}P_{2C}P_{1L} \rangle , \tag{4.2}$$

$$W_{00} = \langle \tfrac{1}{2}(1 - P_{2L})P_{1C} \rangle + \langle \tfrac{1}{2}(1 - P_{1L})P_{2C} \rangle . \tag{4.3}$$

The angular brackets in Eqs. (4.1)–(4.3) indicate an average over the impact parameters of one of the fragments and over the spatial orientation of the molecule.

Equations (4.1)–(4.3) yield different results corresponding to different limiting situations. The limiting situations are as follows:

1. Passage through a thick foil

In this case, there are many collisions and charge exchanges, and therefore there is little dependence on the incoming charge state. The average charge state of fragments from H_2^+ traversing a very thick foil is equal to that of protons or neutral hydrogen atoms traversing the same foil (molecular effects appear only in a thin foil[5]). The particles are independent and the probabilities factor [e.g., $\langle (1 - P_{1C})P_{2L} \rangle = \langle (1 - P_{1C}) \rangle \langle P_{2L} \rangle$]. As for H^+ and H^0 beam traversing the foil, the probability for no-capture by a charged fragment is equal to the loss probability of a neutral one: $\langle (1 - P_{1C}) \rangle = \langle P_{2L} \rangle$, etc. Substituting into Eqs. (4.1)–(4.3), we readily obtain

$$W_{++} = \langle P_{2L} \rangle^2 , \tag{4.4}$$

$$W_{0+} = 2\langle P_{2L} \rangle \langle P_{1C} \rangle , \tag{4.5}$$

$$W_{00} = \langle P_{1C} \rangle^2 , \tag{4.6}$$

$$W_{+} = \langle P_{2L} \rangle , \tag{4.7}$$

$$W_{0} = \langle P_{1C} \rangle , \tag{4.8}$$

where the average indicated by the brackets includes an averaging over many collisions. For this case, in which the particles are independent, the following two correlation factors will vanish:

$$R_1 = \frac{W_+ W_0 - W_{0+}/2}{W_+ W_0 + W_{0+}/2} , \tag{4.9}$$

$$R_2 = \frac{W_{00} W_{++} - (W_{0+}^2)/4}{W_{00} W_{++} + (W_{0+}^2)/4} . \tag{4.10}$$

The experiments show that R_1 and R_2 do not vanish. The value of R_1 is small and is about -0.1 above 400 keV. The value of R_2 varies between -0.6 at 300 keV to -0.9 at 900 keV. Hence, there are correlations between the two fragments and their charge states are not independent.

Figure 6 shows that these correlations exist even in a gaseous target of thickness 0.2 $\mu g/cm^2$ and probably also after collisions in thin foils.[5]

2. Spectator particle case

Suppose that whenever fragment No. 1 is exchanging charge so that either $P_{1L} \neq 0$ or $P_{1C} \neq 0$, fragment No. 2 is outside the dissociation region and cannot exchange charge (thus, $P_{2C} = P_{2L} = 0$). In our projectiles energy range we also have very low electron-capture probability $P_{1L} \sim 1$, $P_{1C} \sim 0$. Therefore Eqs. (4.1)–(4.3) yield

$$W_{++} = \tfrac{1}{2}\langle P_{1L} \rangle \lesssim \tfrac{1}{2} \tag{4.11}$$

$$W_{00} = \tfrac{1}{2}\langle P_{1C} \rangle \sim 0 \tag{4.12}$$

$$W_{0+} = \tfrac{1}{2}\langle 2 - P_{1C} - P_{1L} \rangle \sim \tfrac{1}{2} \tag{4.13}$$

Using these expressions, we get $W_+ \sim \frac{3}{4}$ and $W_0 \sim \frac{1}{4}$. When obtaining these results, one should note that the particles here are not equivalent because particle No. 2 does not participate in the charge exchange process. The results summarized in (4.11)–(4.13) are similar to those obtained for the dissociation of H_2^+ in an H_2 target, and it is reasonable to assume that the dissociation mechanism in the case is indeed of this nature; i.e., one particle is a spectator when the other one exchanges charge.

C. Semiempirical geometrical model for the dissociation process

The probabilities for capture and loss of electrons in the equations for dissociation given above can be calculated by a semiempirical geometrical model.

In this model we assume that the dissociation region may be characterized by a sharply defined radius R_0 around the target atom. Every fragment entering this region may exchange charge, whereas a fragment that does not enter cannot exchange any charge. In the extreme case, any fragment which enters the dissociation region emerges positively charged.

The dissociation problem is then simplified and becomes analogous to the problem of the probability of passing a rod of length d through a ring of radius R_0, when the center of mass of the rod and its orientation are random. The problem was

solved exactly numerically, and for any practical purpose we may write $G(2,2)$ the probability of two rod ends (out of two) passing inside the ring, as

$$G(2,2) \sim e^{-d/R_0}. \tag{4.14}$$

This expression is 4% less than the exact result for $d/R_0 = 2$. For other values of d/R_0, the approximation is closer to the exact result. In the dissociation case, d is the intramolecular distance, R_0 the dissociation radius, and $G(2,2)$ the probability that two fragments (out of two) pass inside the dissociation region. For the extreme dissociation case when no neutral fragments come out of the dissociation region, we get: $W_{00} = 0$, $W_{0+} = \frac{1}{2}(1 - e^{-d/R_0})$, and $W_{++} = \frac{1}{2}(1 + e^{-d/R_0})$. For reasonable values of d/R_0 we obtain values for W_{0+} which are not far from the high energy values in air and Ar targets. However, the energy dependence is wrong, because capture probabilities have not been taken into account.

A possible estimate of the electron capture probability may be obtained by using a universal function for relative average ionization after traversing a foil.[8] This function is well known both experimentally and analytically. For a projectile of velocity V we define the function $F_0(V, Z_1)$ as the relative average number of electrons accompanying an outgoing particle of atomic number Z_1. For $Z_1 > 1$, it is given by the analytical expression[8]

$$F_0(V, Z_1) = \exp(-V/V_0 Z_1^{0.45}), \quad Z_1 > 1 \tag{4.15}$$

For $Z_1 = 1$, the analytic formula (4.15) does not reproduce the experimental results, and the latter are used in our calculations for this case.

We found that the best fit to all the experimental results is obtained by using the following rules: (i) When both fragments enter the dissociation region, $Z_1 = 2$, one fragment affects the electron capture probability of the other. (ii) For a positively charged external fragment, $Z_1 = 2$, the external fragment affects the electron capture probability of the internal one. (iii) For a neutral external fragment, there is no influence and $Z_1 = 1$.

The probability of coming out without an electron after entering the dissociation region is the relative average ionization, $1 - F_0(V, Z_1)$.

Defining $G(2,1)$ as the probability for one fragment being inside the dissociation region while the other is outside [i.e., the complement of $G(2,2)$] we have

$$W_{00} = G(2,2) F_0(V,2)^2 + \tfrac{1}{2} G(2,1) F_0(V,1), \tag{4.16}$$

$$W_{0+} = G(2,2) 2F_0(V,2)[1 - F_0(V,2)] + \tfrac{1}{2} G(2,1)[1 - F_0(V,1)] + \tfrac{1}{2} G(2,1) F_0(V,2), \tag{4.17}$$

$$W_{++} = G(2,2)[1 - F_0(V,2)]^2 + \tfrac{1}{2} G(2,1)[1 - F_0(V,2)]. \tag{4.18}$$

Because F_0 vanishes for high incoming energies, we can find $G(2,2)$ and $G(2,1)$ from the results of Berkner *et al.*[6] without fitting any parameters. However, we preferred to use $G(2,2)$ as an adjustable parameter (this is equivalent to changing d/R_0).

The fit of the model for H_2 with $G(2,2) = 0$ is shown by a solid line in Fig. 5. The fit is good at the higher energies. A fit to the results of Ref. 6 gives a consistent value $G(2,2) = 0.05$. At low energies the theoretical curves do not reproduce the experimental results. If we assume that the external fragment does not influence the internal one, we get in the whole energy region $W_{0+} = 0.50$.

The results for the other gases can be reproduced only by assuming a mutual influence of the fragments when both are in the dissociation region. However, the results may be also fitted without assuming that the external fragment influences the internal one. Only the result for H_2 clearly indicate such an influence.

The model calculation assuming such an influence is shown as a solid line in Fig. 4, for $G(2,2) = 0.50(5)$. A fit to the results of Ref. 6 yields a consistent value $G(2,2) = 0.49$ for an Ar target. This value means $d/R_0 = 0.7$. Assuming an average intramolecular distance $d = 1.3$ Å (Ref. 9), we get $R_0 = 1.7$ Å, in good agreement with the average radius of the external shell of Ar (Ref. 10).

Theoretical calculations of cross sections for various dissociation channels using the Born approximation and the Gryzinski model are presented in Refs. 6 and 4. Their agreement with the experimental data is not too good. It appears that the geometric dissociation model, concentrating directly on charge state distributions and using only one adjustable parameter, is able to reproduce the experimental data much more accurately.

ACKNOWLEDGMENTS

We would like to thank Sh. Gordon, M. Miron, I. Gertner, J. Kantor, J. Saban, and J. Shlomi for their help in the performance of the experimental part of the work.

[1]H. Tawara and A. Russek, Rev. Mod. Phys. 45, 178 (1973).
[2]B. Meierjohann and M. Vogler, J. Phys. B 9, 1801 (1976).
[3]D. R. Sweetman, Proc. R. Soc. A 256, 416 (1960); L. I. Pivovar, V. M. Tubaev, and M. T. Novikov, Zh. Eksp. Teor. Fiz. 40, 34 (1961) [Sov. Phys.-JETP 13, 23 (1961)]; I. Alvarez, C. Cisneros, C. F. Barnett, and J. A. Ray, Phys. Rev. A 14, 602 (1976); H. S. W. Massey, E. H. S. Burhop, and H. B. Gilbody, *Electronic and Ionic Impact Phenomena* (Oxford University, London, 1974), Vol. 4.
[4]J. M. Peek, T. A. Green, and W. H. Weihofen, Phys. Rev. 160, 117 (1967); M. Gryzinski, Phys. Rev. 138, A336 (1965); K. H. Berkner, S. N. Kaplan, R. V. Pyle, and J. W. Stearns, Phys. Rev. 146, 9 (1966).
[5]B. T. Meggit, K. G. Harrison, and M. W. Lucas, J. Phys. B 6, L362 (1973); W. S. Bickel, Phys. Rev. A 12, 1801 (1975).
[6]K. H. Berkner, S. N. Kaplan, R. V. Pyle, and J. W. Stearns, Phys. Rev. 146, 9 (1966).
[7]L. H. Toburen, Phys. Rev. A 3, 216 (1971); L. H. Toburen and W. E. Wilson, Phys. Rev. A 5, 247 (1972); W. E. Wilson and L. H. Toburen, Phys. Rev. A 7, 1585 (1973).
[8]H. D. Betz, Rev. Mod. Phys. 44, 465 (1972).
[9]W. Brandt, Nucl. Instrum. Methods 132, 43 (1976).
[10]C. C. Lu, T. A. Carlson, F. B. Malik, T. C. Tucker, and C. W. Nestor, At. Data 3, 1 (1971); J. P. Desclaux, At. Data Nucl. Data Tables 12, 312 (1973).